Quantitative description for the growth rate of self-induced GaN nanowires

V. Consonni,[1,2,*] V. G. Dubrovskii,[3,4] A. Trampert,[1] L. Geelhaar,[1] and H. Riechert[1]

[1]*Paul-Drude-Institut für Festkörperelektronik, Hausvogteiplatz 5-7, 10117 Berlin, Germany*

[2]*Laboratoire des Matériaux et du Génie Physique, CNRS—Grenoble INP, 3 parvis Louis Néel 38016 Grenoble, France*

[3]*St. Petersburg Academic University, Khlopina 8/3, 194021 St. Petersburg, Russia*

[4]*Ioffe Physical Technical Institute of the Russian Academy of Sciences, Politekhnicheskaya 26, 194021 St. Petersburg, Russia*

(Received 2 February 2012; revised manuscript received 6 March 2012; published 12 April 2012)

We determine with high precision the growth rate of self-induced GaN nanowires grown by molecular beam epitaxy under various conditions from scanning electron micrographs by taking into account *in situ* measurements of the initial incubation time, which is needed before the nanowire growth starts. In order to quantitatively describe the dependence of the growth rate on growth time, gallium flux, and growth temperature, we develop a detailed theoretical model of diffusion-induced nanowire growth specifically for the self-induced approach, i.e., without any droplet at the nanowire top. The theoretical fits are in excellent agreement with the experimental data and allow us to deduce important kinetic parameters of the self-induced GaN nanowire growth. The gallium adatom effective diffusion length on the nanowire sidewalls composed of *m*-plane facets is only 45 nm, which is consistent with our experimental finding that the growth rate initially decreases drastically as the contribution from the adatoms on the planar substrate surface rapidly vanishes. In contrast, the gallium adatom effective diffusion length on the amorphous silicon nitride substrate surface reaches about 100 nm. Furthermore, the nucleation energy on the nanowire sidewalls is found to be 5.44 eV and is larger than on their top facet accounting for the nanowire elongation.

DOI: 10.1103/PhysRevB.85.155313 PACS number(s): 81.15.Hi, 62.23.Hj, 81.05.Ea

I. INTRODUCTION

The self-induced growth of GaN nanowires (NWs) by molecular beam epitaxy (MBE) is a promising approach for the fabrication of low-cost light-emitting diodes on silicon.[1–6] A highly nitrogen-rich vapor phase is required and often combined with a high substrate temperature for their self-induced formation.[7–15] Very importantly, a clear distinction is necessary between the initial nucleation phase that results in the NW nucleus formation and the subsequent growth phase that leads to the NW nucleus elongation. It has recently been shown that the self-induced formation of GaN NW nuclei occurs through the shape transitions of pre-existing islands beyond a critical radius.[16,17] The anisotropy of surface energy has been identified as the predominant driving force, and the nucleation phase is therefore expected to be driven by thermodynamics.[16,17]

Subsequently, the NW nucleus elongation takes place. In contrast to the nucleation phase, the growth phase is expected to be dominated by kinetics.[18] For technological applications, the control of the NW morphology and the optimal growth conditions are crucial, for instance, to select the highest growth rate. However, for the self-induced approach, the physical process at work during the growth phase is still not completely understood. Similarly to the catalyst-induced approach, it has been suggested for the self-induced approach that the direct impinging flux on the NW top facet as well as the adatom surface diffusion on the substrate and along the NW vertical sidewalls are involved.[14,15,19–25] Furthermore, the geometrical characteristics in the MBE chamber also play a significant role because the gallium and nitrogen fluxes directly depend on the angles of the effusion cell and plasma source with respect to the substrate.[26,27] However, the ratio between the incorporation rates on the NW top facet and on its vertical sidewalls as well as a detailed understanding of the diffusion mechanisms are still open questions. Additionally, a quantitative description of the growth phase is still lacking. Some elementary theoretical models have already been used on the basis of the catalyst-induced approach although the self-induced approach has very specific characteristics. These models do not lead to a deep understanding of the growth phase, and we substantially extend them, which allow us to extract much more of the essential parameters that describe the self-induced NW growth.[19,27–29]

The aim of this paper is to investigate both experimentally and theoretically the evolution of the NW mean growth rate with the growth time, gallium flux, and growth temperature. Experimentally, the NW mean growth rate is determined from the NW length and the total growth time. Thus, compared to the use of AlN markers inserted into GaN NWs,[22,27] any foreign material that may strongly influence the growth phase during which the NW elongation proceeds is avoided. Very importantly, in order to deduce the NW mean growth rate with high precision, we have taken into account the incubation time in the total growth time by distinguishing between the nucleation and growth phases using *in situ* reflection high-energy electron diffraction (RHEED) measurements.[30] This aspect is crucial because the incubation time significantly depends on both the gallium flux and growth temperature and can widely vary from several tens of seconds to several tens of minutes.[30] A theoretical modeling based on the diffusion-induced NW growth is further developed specifically for the self-induced approach and is in very good agreement with the experimental data. The theoretical model allows the determination of a wide number of kinetic parameters of the self-induced GaN NW growth.

II. EXPERIMENT

GaN NWs were grown on Si(111) substrates by plasma-assisted MBE. The active nitrogen species and gallium atoms

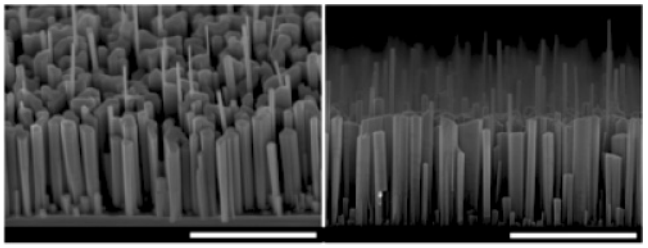

FIG. 1. Tilted (left) and cross-sectional (right) FESEM images of GaN NWs grown for 3 h at a substrate temperature and gallium rate of 780 °C and 0.45 Å/s, respectively. Note that the scale bar is 1 μm.

were supplied by a plasma source and by an effusion cell, respectively. The angles of the gallium effusion cell and of the nitrogen plasma source with respect to the substrate normal are 21 and 33°, respectively. Prior to GaN NW growth, the substrates were exposed to an active nitrogen flux for 5 min, resulting in the formation of a continuous Si_xN_y amorphous interlayer with a thickness of about 2 nm. The nominal gallium and nitrogen rates correspond to the growth rate of GaN planar layers deposited on SiC(111) substrates under nitrogen- and gallium-rich conditions, respectively. The growth temperature and gallium rate were varied in the ranges of 770 to 815 °C and 0.25 to 0.7 Å/s, respectively. The nitrogen rate was equal to 2.8 Å/s, yielding a V/III ratio in the range of 4 to 11.2. *In situ* RHEED measurements were performed with an incident electron beam angle to the substrate of 3°. As discussed in Ref. 30, the total growth time for the self-induced approach is the sum of the incubation time necessary for the nucleation of spherical cap-shaped islands, of the transition time required for the shape transition to NWs, and of the actual (i.e., elongation) growth time corresponding to the growth phase. Very importantly, the total growth time was adjusted for each experiment such that the sum of the transition and actual growth times (i.e., denoted as the pseudoactual growth time) was systematically 3 h: the gallium shutter was closed 3 h after the end of the incubation stage as indicated by the appearance of GaN three-dimensional spots in RHEED. In other words, the transition time of typically several seconds to several minutes and its dependence on the growth conditions is considered as negligible with respect to the actual growth time for the gallium rate and growth temperature series.[17] The NW mean growth rate was, therefore, experimentally measured with high precision as the ratio between the NW length L and the pseudoactual growth time $t_{\mathrm{pseudoactual}}$, as follows: $dL/dt = L/t_{\mathrm{pseudoactual}}$. The NW length L was assessed among a population of more than 50 NWs from cross-sectional field-emission scanning electron microscopy (FESEM) images, as shown in Fig. 1.

Another series of samples was grown for different growth durations at a substrate temperature and gallium rate of 780 °C and 0.45 Å/s, respectively. For these growth conditions, the incubation time was found to be 6.5 min as shown by the appearance of GaN three-dimensional spots in RHEED. Additionally, the transition time was determined by performing transmission electron microscopy (TEM) imaging on all the samples of the growth time series. While only spherical cap-shaped islands are initially formed, it was revealed that the very first NWs are nucleated after about 5 min following the appearance of GaN three-dimensional spots in RHEED:[17] this strongly indicates that the transition time was about 5 min under such growth conditions. As a result, the actual growth time between 270 and 22770 s is considered here for this series instead of the pseudoactual growth time for the gallium rate and growth temperature series. The NW mean growth rate was further experimentally deduced with high precision as the ratio between the NW length L and the actual growth time t_{actual}, as follows: $dL/dt = L/t_{\mathrm{actual}}$.

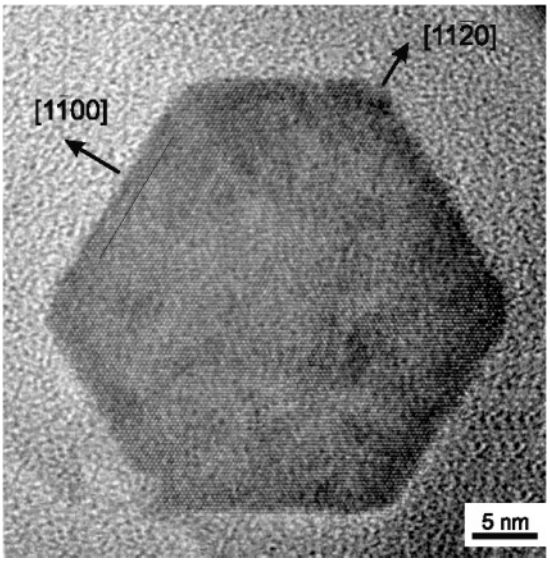

FIG. 2. Top-view HRTEM image of a GaN NW, revealing that the vertical sidewalls are composed of m planes (i.e. (1$\bar{1}$00)planes).

Specimens for top-view TEM imaging were prepared by mechanical lapping and polishing, followed by argon ion milling according to standard techniques. TEM images were acquired with a JEOL 3010 microscope operating at 300 kV. Importantly, the vertical sidewalls are composed of m planes as deduced from the top-view HRTEM image in Fig. 2, which is in agreement with Refs. 20, 21, and 23.

III. RESULTS AND DISCUSSION

A. Theoretical modeling of the NW axial growth rate for the self-induced approach

1. Principles of the theoretical modeling

In the following, the NW axial growth rate is modeled within the approach given by Dubrovskii *et al.*[31–34] and adapted to the case of self-induced GaN NWs. The principles for the theoretical modeling are revealed in the schematic given in Fig. 3.

The elongation of an isolated hexahedral NW is determined by three factors: the direct impingement of nitrogen and gallium fluxes onto its top facet and vertical sidewalls as well as the surface diffusion of adatoms. Under highly nitrogen-rich conditions, the growth kinetics is assumed to be limited by the corresponding gallium fluxes. The gallium beam of intensity J makes the angle α to the substrate normal. From considerations of material balance, the NW growth rate denoted as dL/dt is

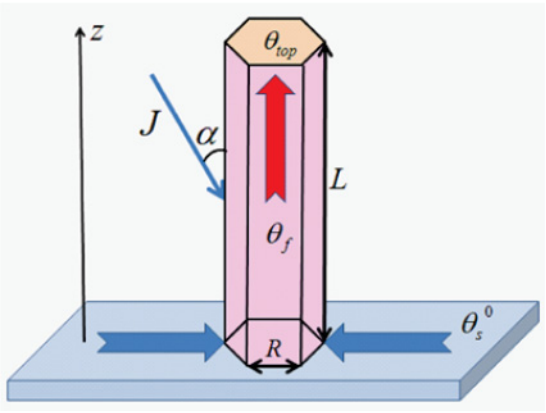

FIG. 3. (Color online) Schematic of the theoretical model for the surface diffusion-induced NW growth in the self-induced approach. The parameters given in the schematic are defined in the text.

given by

$$\frac{3\sqrt{3}R^2}{2\Omega_s}\frac{dL}{dt} = \frac{3\sqrt{3}R^2}{2}(J\cos\alpha - J_{\rm des}) - 6RD_f\left(\frac{dn_f}{dz}\right)_{z=L}, \tag{1}$$

in which R is the radius of the NW cross-section, Ω_s is the elementary volume in the NW, $J_{\rm des}$ is the desorption rate from the NW top facet, D_f and n_f are the diffusion coefficient and concentration of gallium adatoms on the NW vertical sidewalls composed of m planes, respectively. R is assumed as being constant in a first approximation and hence as being independent upon the growth duration and NW length. The net gallium flux contributing to the NW elongation is given on the left-hand side of Eq. (1). On the right-hand side, the first term represents the adsorption-desorption growth rate on the NW top facet, while the second term stands for the diffusion flux of gallium adatoms from the planar substrate surface and NW sidewalls to the NW top.[31,32]

It is expected that $n_f(z)$ obeys the following stationary diffusion equation:[31] $D_f d^2n_f/dz^2 + (J/3)\sin\alpha - n_f/\tau_f = 0$, in which the diffusion flux is balanced by the impingement flux onto the NW sidewalls and the gallium sink with the characteristic lifetime τ_f. The coefficient 1/3 in the arrival rate is the geometrical factor of MBE growth, where the flux sees the projection $2R$, not the entire perimeter $6R$ or, in other words, impinges on only two out of six side facets of a hexahedral NW. The chemical potential of gallium adatoms on the NW sidewalls equals $k_BT\ln\theta_f$, where $\theta_f = \sigma_f n_f \ll 1$ is the surface filling factor, σ_f is the NW sidewall elementary area, T is the surface temperature, and k_B is the Boltzmann constant. We use the following boundary conditions for the diffusion equation as seen in Fig. 3: (i) the equality of the activity of gallium adatoms on the NW sidewalls at $z = L$ to its activity on the NW top facet results in $\theta_f(z = L) = \theta_{\rm top}$; (ii) the equality of the activity of gallium adatoms at the NW base to its activity on the substrate surface is obtained by balancing the arrival rate $J\cos\alpha$ to the sink with the characteristic lifetime τ_s. This leads to $\theta_f(z = 0) = J\tau_s\sigma_s\cos\alpha$, where σ_s is the elementary area on the substrate surface. Such a condition at $z = 0$ is valid when the diffusion length of gallium adatoms on the planar substrate surface is much larger than the NW radius.[35] By solving the diffusion equation for $n_f(z)$ and by calculating the corresponding diffusion flux at $z = L$, Eq. (1) can be reduced to

$$\frac{dL}{dt} = V\left\{1 - \upsilon_{\rm des} + \frac{4}{\sqrt{3}R} \times \left[\frac{(\lambda_s^2/b\lambda_f)g_s + \lambda_f g_f\tan\alpha(\cosh(L/\lambda_f) - 1)}{\sinh(L/\lambda_f)}\right]\right\}. \tag{2}$$

Here, $V = J\Omega_s\cos\alpha$ is the equivalent gallium rate, and $\upsilon_{\rm des} = V_{\rm des}/V$ is the relative desorption rate. The quantities $\lambda_s = \sqrt{D_s\tau_s}$ and $\lambda_f = \sqrt{D_f\tau_f}$ are the effective diffusion lengths on the substrate surface and on the NW sidewalls, respectively, in which D_s is the diffusion coefficient of gallium adatoms on the substrate surface. While the diffusion lengths λ_s^0 and λ_f^0 are defined at equilibrium conditions on island-free bare surfaces, the effective diffusion lengths λ_s and λ_f are the diffusion length as growth proceeds, resulting in $\lambda_s \leqslant \lambda_s^0$ and $\lambda_f \leqslant \lambda_f^0$. $b = (D_s\sigma_f/D_f\sigma_s)$ is a coefficient of the order of one. The parameters $g_s = 1 - \theta_{\rm top}/(J\tau_s\sigma_s\cos\alpha)$ and $g_f = 1 - 3\theta_{\rm top}/(J\tau_f\sigma_f\sin\alpha)$ represent the driving forces for the diffusion of gallium adatoms to the NW top.[32]

Let us now consider some general properties of Eq. (2) that are relevant for the dependence of the NW growth rate on the growth time. At small and large NW lengths L, Eq. (2) has the following asymptotes:

$$\frac{dL}{dt} = V\left\{1 - \upsilon_{\rm des} + \frac{4}{\sqrt{3}R}\left[\frac{\lambda_s^2 g_s}{bL} + \frac{g_f\tan\alpha}{2}L\right]\right\}, \quad L \ll \lambda_f; \tag{3}$$

$$\frac{dL}{dt} = V\left\{1 - \upsilon_{\rm des} + \frac{4\lambda_f}{\sqrt{3}R}g_f\tan\alpha\right\}, \quad L \gg \lambda_f. \tag{4}$$

From Eq. (3), it follows that the NW growth rate at $L \ll \lambda_f$ is independent upon λ_f and comprises three distinct contributions: a constant adsorption-desorption growth rate, the $1/L$ diffusion term originating from the gallium adatoms on the substrate surface, and the L diffusion term coming from the gallium adatoms on the NW sidewalls. From Eq. (4), it turns out that the NW growth rate at $L \gg \lambda_f$ does not contain the contribution from the substrate surface because all the gallium adatoms are either desorbed or trapped by the islands (i.e., steps) on the NW sidewalls before they can reach the NW top. The diffusion term is hence proportional to λ_f/R and does not depend on L.[33,34]

The dependence of the NW growth rate on the gallium rate is linear in the first approximation, where the bracket term in Eq. (2) is independent upon V. It should be pointed out, however, that the effective diffusion lengths generally depend on V, as they may be limited by a process of flux-dependent surface nucleation.[32] The dependence of the NW growth rate on the growth temperature is usually complex,[33,34] and may be qualitatively different at distinct growth durations. We also note that the effective diffusion length of gallium adatoms on the NW sidewalls at typical GaN growth temperatures is small. The value of 40 nm has been reported in Refs. 19 and 27, and our own estimate is given hereafter. Therefore, for sufficiently long NWs, the NW growth rate is roughly given by Eq. (4). By

assuming that the temperature dependence of g_f is weak, the dependence of the NW growth rate on the growth temperature is driven by λ_f and $v_{\rm des}$.

For the former, the approach given in Ref. 33 is used where the effective diffusion length is limited either by the surface nucleation of islands (at low T) or by the desorption (at high T):

$$\lambda_f = \frac{\lambda_f^0}{\sqrt{1 + 2\pi N_{isl}\left(\lambda_f^0\right)^2}}, \tag{5}$$

where $\lambda_f^0 \propto \exp[(E_{\rm des}^f - E_{\rm diff}^f)/2k_BT]$ is the diffusion length of gallium adatoms at equilibrium conditions on an atomically defined and island-free bare surface (with $E_{\rm des}^f$ and $E_{\rm diff}^f$ being the activation energies for the desorption and surface diffusion on the NW sidewalls, respectively) and $N_{isl} \propto V^{3/2}\exp(E_{\rm nucl}^f/k_BT)$ is the island surface density on the NW sidewalls (with $E_{\rm nucl}^f$ being the characteristic nucleation energy barrier).[33,34] By rearranging Eq. (5), one can get the following relation:

$$\lambda_f = \left\{\left[\lambda_f^0(T_*)\right]^{-2}\exp\left[-G_*\left(\frac{T_*}{T}-1\right)\right.\right. \\ \left.\left. + 2\pi N_{isl}(T_*,V_*)\frac{V^{3/2}}{V_*^{3/2}}\exp\left[F_*\left(\frac{T_*}{T}-1\right)\right]\right]\right\}^{-1/2}, \tag{6}$$

in which T_* is the reference temperature, V_* is the reference gallium rate, $G_* = (E_{\rm des}^f - E_{\rm diff}^f)/k_BT_*$, and $F_* = E_{\rm nucl}^f/k_BT_*$.

For the latter, the standard Arrhenius-like approximation is used such that $v_{\rm des} \propto \theta_{\rm top} \propto \exp(-E_{\rm top}/k_BT)$ with the corresponding energy barrier $E_{\rm top}$. The value of $E_{\rm top}$ simultaneously accounts for the surface nucleation and desorption on the NW top facet.[33,34] This can be represented in the form

$$v_{\rm des} = v_{\rm des}(T_*)\exp\left[-C_*\left(\frac{T_*}{T}-1\right)\right], \tag{7}$$

where $C_* = E_{\rm top}/k_BT_*$.

2. *Shadowing effects*

The present theoretical modeling in the last section focuses in an ideal case on the growth rate of an isolated hexahedral NW within the self-induced approach. Still, this approach typically results in most practical cases in the formation of highly dense NW ensembles as shown in Fig. 1, which can lead to shadowing effects between NWs. The shadowing effects are dependent upon the geometrical parameters such as both the NW density and radius (i.e., NW spacing) and the gallium beam angle.[36] Let us consider a NW ensemble distributed in a regular square area. By taking a typical NW density and radius of 100 μm^{-2} and 30 nm,[12,28,37] the NW spacing is about 51 nm. In other words, the gallium beam with an angle of 21°, for instance, impinges on a NW height of 133 nm, which is much larger than the effective diffusion length of about 40–45 nm as reported in Refs. 19 and 27 and as deduced hereafter. More importantly, a critical NW density and gallium beam angle can be determined by equating the effective diffusion length of 45 nm with the impinged NW height. First, by taking a NW density and radius of 100 μm^{-2} and 30 nm, a critical gallium beam angle of 49° is found: in brief, shadowing effects can be neglected for a gallium beam angle smaller than 49°, which is quite common in the MBE chamber. Inversely, by taking a NW radius of 30 nm and a gallium beam angle of 21°, a critical NW density of about 200 μm^{-2} is deduced, which is high with respect to the typical NW density. As a consequence, although shadowing effects can play a significant role, the present theoretical modeling can account for the NW growth rate in most practical cases and especially for the forthcoming experimental results because the effective diffusion length of gallium adatoms on the NW sidewalls is fairly short.

B. Influence of the growth conditions on the NW growth rate

The evolution of the NW mean growth rate with the NW length, gallium rate, and growth temperature is presented in Figs. 4–6. Interestingly, the NW mean growth rate is systematically larger than the gallium rate but smaller than the nitrogen rate, showing that the surface diffusion of gallium adatoms on the substrate and then along the NW vertical sidewalls to their top does play a significant role as discussed in our theoretical model.

1. *Effects of the growth time*

The evolution of the NW mean growth rate as a function of the NW length at fixed $T = 780\,^{\circ}$C and $V = 0.45$ Å/s is presented in Fig. 4. The NW mean growth rate for the NW length of about 50 nm reveals that the nucleation events spread over a certain time as shown by the large error bars. As the NW length increases from about 50 to 880 nm (corresponding to the increase in the actual growth time from 270 to 11070 s), the NW mean growth rate initially decreases drastically. Subsequently, for the NW length larger than 880 nm (corresponding to the actual growth time longer than 11070 s), the NW mean growth rate slightly increases from 0.79 to 0.95 Å/s. It should be noted that the opposite trend has been reported in Refs. 12 and 24, indicating the deleterious effect of not considering the incubation and transition times.

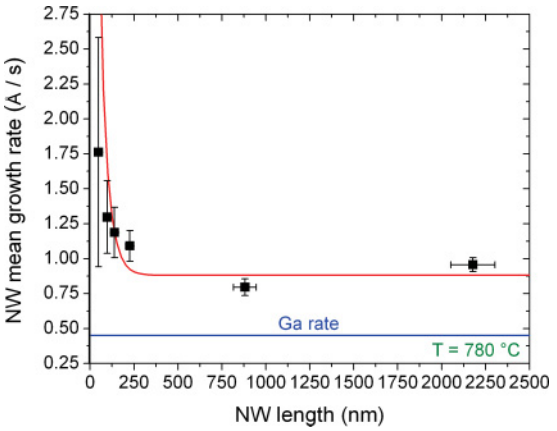

FIG. 4. (Color online) Evolution of the NW mean growth rate as a function of the NW length: dots–experimental data, red (dark gray) line—theoretical fit obtained from Eq. (2) with $\lambda_f = 45$ nm, $g_f = 0.794$, $v_{\rm des} = 0.1$, $\sqrt{g_s}\lambda_s = 70$ nm, and $R = 30$ nm. The blue (medium gray) line indicates the value of the gallium rate.

Even when a constant incubation time is taken into account while the transition time is ignored, the NW mean growth rate is not deduced so precisely, and the opposite trend has been stated in Ref. 27, which is likely due to geometrical effects. Some significant effects could also arise from the use of AlN markers that cover the NW vertical sidewalls and hence affect the adatom incorporation and diffusion properties. In brief, the experimental dependence of the NW mean growth rate on the NW length is overall well fitted by Eq. (2). The fit shown in Fig. 4 is obtained with the following parameters: $\lambda_f = 45$ nm, $g_f = 0.794$, $v_{\rm des} = 0.1$, $\sqrt{g_s}\lambda_s = 70$ nm, and $R = 30$ nm, at the gallium incident angle $\alpha = 21^\circ$. The value of λ_f of 45 nm at 780 °C is consistent with the reported value of 40 nm according to Refs. 19 and 27 and is typical for the self-induced growth of GaN NWs. In other words, this indicates that the contribution from the planar substrate surface is much less pronounced. The value of λ_s of the order of 100 nm justifies the assumption made in the derivation of the growth equation: the diffusion length of gallium adatoms on the substrate surface is indeed much larger that the NW radius of 30 nm. Also, our value for λ_s is significantly smaller than the estimate of 400 nm deduced from experimental results on prepatterned substrates.[29] Because no growth of a parasitic two-dimensional surface layer is observed in our case, λ_s should be limited by the surface density of both spherical cap-shaped islands and NWs in contrast to the growth on prepatterned substrates for which the mechanisms are distinct. It should be noted that the NW mean growth rate is much larger than the gallium deposition rate in the beginning. The saturation limit predicted by the theoretical model at 0.88 Å/s corresponds to the asymptote at $L \gg \lambda_f$ as given by Eq. (4), where the contribution from the diffusion of gallium adatoms on the substrate surface vanishes. This value is also noticeably higher than the gallium rate, thus demonstrating that the adsorption and diffusion of gallium adatoms on the vertical sidewalls significantly contributes to the NW elongation. Such a contribution is fairly weak for short actual growth time (i.e., short NWs are mainly fed from the substrate surface) but is drastically strengthened with respect to the substrate gallium adatoms as the NW elongation proceeds (i.e., long NWs are no longer fed from the substrate surface). This shows the very strong importance of geometrical effects on the sidewall deposition, as mentioned in Refs. 26 and 27, because the gallium impinging flux on the NW vertical sidewalls directly depends on the angle between the substrate and the gallium effusion cell. The slight discrepancy in the NW mean growth rate between the fit that predicts a saturation limit and the experimental results that shows a slight increase for the NW length larger than 880 nm points out the importance of the coalescence process for very long NWs, which is not considered in the present theoretical model.

2. *Effects of the gallium rate*

In the following, the pseudoactual growth time of 3 h is systematically selected, and because λ_f is small, the NW mean growth rate can be fitted by Eq. (4) at $L \gg \lambda_f$. The evolution of the NW mean growth rate is presented as a function of the gallium rate in Fig. 5. As the gallium rate is increased between 0.25 and 0.7 Å/s, the NW mean growth rate continuously rises from 0.42 to 1.12 Å/s. Its experimental dependence is again

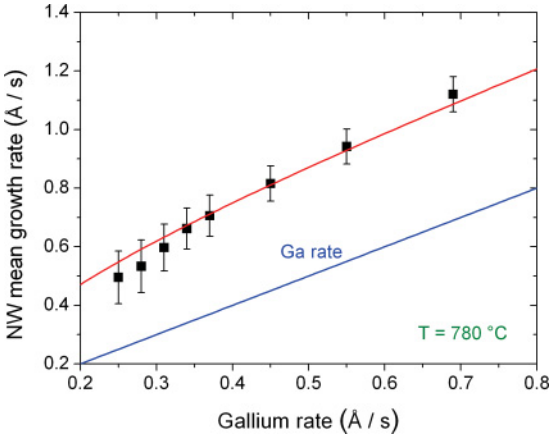

FIG. 5. (Color online) Evolution of the NW mean growth rate as a function of the gallium rate: dots—experimental data, red (dark gray) line—theoretical fit obtained from Eqs. (4) and (6) with $\lambda_f = 45$ nm, $g_f = 0.794$, $v_{\rm des} = 0.1$, $R = 30$ nm, $\lambda_f^0(T_*, V_*) = 118$ nm, and $N_{isl}(T_*, V_*) = 6 \times 10^{-5}$ nm^{-2} at the reference values $T_* = 780$ °C and $V_* = 0.45$ Å/s. The blue (medium gray) line indicates the value of the gallium rate.

in good agreement with the theoretical model and well fitted by Eqs. (4) and (6). The fit shown in Fig. 5 is obtained with the following parameters: $\lambda_f = 45$ nm, $g_f = 0.794$, $v_{\rm des} = 0.1$, $R = 30$ nm, $\lambda_f^0(T_*, V_*) = 118$ nm, and $N_{isl}(T_*, V_*) = 6 \times 10^{-5}$ nm^{-2} at the reference values $T_* = 780$ °C and $V_* = 0.45$ Å/s. It is expected that a larger amount of gallium adatoms is involved in the adsorption and diffusion contribution to the growth rate as the gallium rate is increased. Therefore, the NW mean growth rate is higher at a larger gallium rate. The dependence presented in Fig. 5 is not completely linear in contrast to Refs. 9, 12, and 15. A small deviation from the linearity towards higher gallium rates can be accounted for by a more efficient surface nucleation of islands at the NW vertical sidewalls as given in Eq. (6). These results strongly suggest that the GaN NW growth should be performed at very high gallium rate. Still, increasing the gallium rate at a given nitrogen rate is not conceivable because the NW nuclei would not be formed.[16,17] Indeed, the NW nuclei are formed following the shape transitions from pre-existing three-dimensional islands, which are energetically favorable due to an energy balance in favor of the NW morphology only in a certain range of gallium rate (i.e., V/III ratio).[16,17] Also, even during the growth stage, the gallium rate cannot be increased deliberately because this would eventually lead to an enhancement of radial growth, and the NW morphology would be lost.[38]

3. *Effects of the growth temperature*

More importantly is the dependence of the NW mean growth rate on growth temperature, as depicted in Fig. 6. The evolution of the NW mean growth rate follows two consecutive steps: (i) the NW mean growth rate initially increases to 0.86 Å/s as the growth temperature is raised from 770 to 795 °C and (ii) subsequently decreases rapidly for higher growth temperatures. It should be noted that the initial increase in the NW mean growth rate is more significant than the

increase reported in Ref. 25: this may be due to the critical increase in the incubation time with the growth temperature, which could lead to an overestimation of the NW mean growth rate at low growth temperatures. The occurrence of a maximum NW mean growth rate for intermediate growth temperatures is of high interest for technological applications in which the highest NW mean growth rate is required. Interestingly, a maximum NW density has also been reported at about 785 °C,[37] which points out that such a growth temperature is optimal for the NW morphology. The experimental dependence of the NW mean growth rate on the growth temperature is again very well fitted by Eqs. (4), (6), and (7). The fit shown in Fig. 6 is obtained with the same values of parameters as for the growth time and gallium rate dependences at $v_{\mathrm{des}}(T_*) = 0.1$, $G_* = 28$, $F_* = 60$, and $C_* = 80$. The obtained value of G_* leads to $E^f_{\mathrm{des}} - E^f_{\mathrm{diff}} = 2.54$ eV, which is in very good accordance with the available data on the activation energies. In GaN, the diffusion barrier for gallium adatoms on the NW vertical sidewalls composed of m planes is 0.21 eV,[39] which reveals that $E^f_{\mathrm{diff}} = 0.21$ eV and hence that $E^f_{\mathrm{des}} = 2.75$ eV. No value for the activation energy of desorption of gallium adatoms on the GaN m planes has so far been reported, but it should be noted that the corresponding activation energy lies in the typical range of about 2 to 5.1 eV on the GaN c plane.[40–43] Consequently, the value of 2.75 eV for E^f_{des} seems quite reasonable. The values of F_* and C_* result in $E^f_{\mathrm{nucl}} = 5.44$ eV and $E_{\mathrm{top}} = 7.26$ eV. The former is noticeably larger, showing that the nucleation barrier on the NW vertical sidewalls is twice higher than the activation energy of desorption of gallium adatoms. Also, the value is close to the nucleation energy of spherical cap-shaped islands on the Si_xN_y amorphous interlayer, which is again reasonable.[30] The higher value of E_{top} is most likely due to the fact that it simultaneously accounts for the surface nucleation and desorption. Interestingly, the desorption activation energy

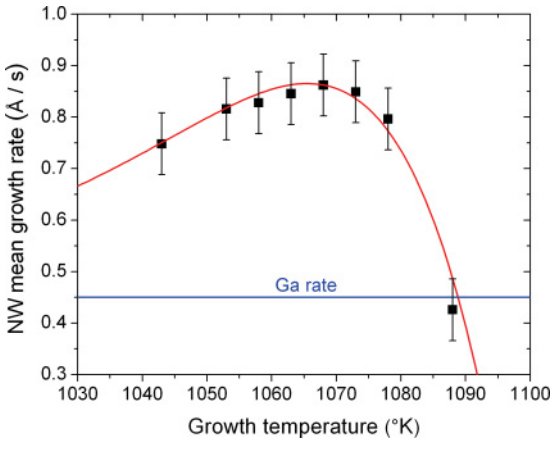

FIG. 6. (Color online) Evolution of the NW mean growth rate as a function of the substrate temperature: dots—experimental data, red (dark gray) line—theoretical fit obtained from Eqs. (4), (6), and (7) with $\lambda_f = 45$ nm, $g_f = 0.794$, $v_{\mathrm{des}} = 0.1$, $R = 30$ nm, $\lambda^0_f(T_*, V_*) = 118$ nm, and $N_{isl}(T_*, V_*) = 6 \times 10^{-5}$ nm^{-2} at the reference values $T_* = 780$ °C and $V_* = 0.45$ Å/s, $v_{\mathrm{des}}(T_*) = 0.1$, $G_* = 28$, $F_* = 60$, and $C_* = 80$. The blue (medium gray) line indicates the value of the gallium rate.

on the GaN c plane is expected to be larger than 2 eV.[40–43] As a result, the nucleation barrier is lower on the NW top facet than on their vertical sidewalls, such that GaN NWs elongate much faster in the axial direction than they grow in the radial direction. It is further worth noticing that the surface diffusion of gallium adatoms along the NW vertical sidewalls is enhanced by raising the growth temperature, whereby a larger amount of gallium adatoms reaches the NW top. Still, the gallium desorption from the NW top facet and vertical sidewalls may be prevalent for growth temperatures higher than 790 °C, accounting for the eventual decrease in the NW mean growth rate.

IV. CONCLUSION

In summary, the growth rate of self-induced GaN NWs by MBE has comprehensively been determined. This was experimentally achieved by cross-section view FESEM images, taking into account the incubation time for the initial nucleation of spherical cap-shaped islands. The evolution of the growth rate with the growth time, gallium rate, and growth temperature has quantitatively been described within a theoretical model based on the surface diffusion-induced NW growth for the self-induced approach. The NW elongation is strongly governed by the direct impinging flux on their top facet and by the adatom adsorption and diffusion on their vertical sidewalls composed of m planes as shown by HRTEM imaging. The shadowing effects have been discussed in terms of geometrical constraints in the NW ensembles. The experimental dependences on the growth time, gallium rate, and growth temperature are refined and present distinctly different features with respect to the literature, pointing out the importance of taking the incubation time into account. Additionally, the experimental data are in very good agreement with the theoretical model we have specifically developed for the self-induced growth of GaN NWs. One single set of identical fitting parameters allows to fit all the experimentally observed dependences, which is strong evidence for the accuracy of our model. Important kinetic parameters have been deduced from the theoretical fits such as the effective diffusion length for the gallium adatoms of about 45 nm on the NW vertical sidewalls and of about 100 nm on the Si_xN_y amorphous interlayer. The contribution from the adatoms on the planar substrate surface thus rapidly vanishes during the elongation process, showing that the gallium flux impinging on the NW sidewalls becomes predominant and hence that geometrical effects are critical. Very importantly, it is found that the nucleation energy equals 5.44 eV on the NW vertical sidewalls and is larger than on their top facet accounting for the NW elongation.

ACKNOWLEDGMENTS

This work was partly supported by the German BMBF joint research project MONALISA (Contract No. 01BL0810), contracts with the Russian Ministry of Education and Science, grants of Russian Foundation for Basic Research and FP7 projects SMASH (Contract No. 228999), SOBONA (Contract No. 268154) and FUNPROBE (Contract No. 269169). The authors thank A.K. Bluhm and M. Knelangen for their experimental assistance in SEM and TEM imaging as well as O. Brandt for helpful discussions.

*vincent.consonni@grenoble-inp.fr

[1] A. Kikuchi, M. Kawai, M. Tada, and K. Kishino, Jpn. J. Appl. Phys. **43**, L1524 (2004).

[2] A.-L. Bavencove, G. Tourbot, E. Pougeoise, J. Garcia, P. Gilet, F. Lévy, B. André, G. Feuillet, B. Gayral, B. Daudin, and Le Si Dang, Phys. Status Solidi A **207**, 1425 (2010).

[3] H.-W. Lin, Y.-J. Lu, H.-Y. Chen, H.-M. Lee, and S. Gwo, Appl. Phys. Lett. **97**, 073101 (2010).

[4] R. Armitage and K. Tsubakin, Nanotechnology **21**, 195202 (2010).

[5] W. Guo, M. Zhang, P. Bhattacharya, and J. Heo, Nano Lett. **11**, 1434 (2011).

[6] H. P. T. Nguyen, S. Zhang, K. Cui, X. Han, S. Fathololoumi, M. Couillard, G. A. Botton, and Z. Mi, Nano Lett. **11**, 1919 (2011).

[7] M. Yoshizawa, A. Kikuchi, M. Mori, N. Fujita, and K. Kishino, Jpn. J. Appl. Phys. **36**, L459 (1997).

[8] M. A. Sanchez-Garcia, E. Calleja, E. Monroy, F. J. Sanchez, F. Calle, E. Muñoz, and R. Beresford, J. Cryst. Growth **183**, 23 (1998).

[9] Y. S. Park, S.-H. Lee, J.-E. Oh, C.-M. Park, and T.-W. Kang, J. Cryst. Growth **282**, 313 (2005).

[10] R. Meijers, T. Richter, R. Calarco, T. Stoica, H.-P. Bochem, M. Marso, and H. Lüth, J. Cryst. Growth **289**, 381 (2006).

[11] K. A. Bertness, A. Roshko, N. A. Sanford, J. M. Barker, and A. V. Davydov, J. Cryst. Growth **287**, 522 (2006).

[12] R. Songmuang, O. Landré, and B. Daudin, Appl. Phys. Lett. **91**, 251902 (2007).

[13] M. Tchernycheva, C. Sartel, G. Cirlin, L. Travers, G. Patriarche, J.-C. Harmand, Le Si Dang, J. Renard, B. Gayral, L. Nevou, and F. Julien, Nanotechnology **18**, 385306 (2007).

[14] J. Ristíc, E. Calleja, S. Fernández-Garrido, L. Cerutti, A. Trampert, U. Jahn, and K. H. Ploog, J. Cryst. Growth **310**, 4035 (2008).

[15] S. Fernández-Garrido, J. Grandal, E. Calleja, M. A. Sánchez-García, and D. López-Romero, J. Appl. Phys. **106**, 126102 (2009).

[16] V. Consonni, M. Knelangen, L. Geelhaar, A. Trampert, and H. Riechert, Phys. Rev. B **81**, 085310 (2010).

[17] V. Consonni, M. Hanke, M. Knelangen, L. Geelhaar, A. Trampert, and H. Riechert, Phys. Rev. B **83**, 035310 (2011).

[18] J. Johansson, C. Patrik, T. Svensson, T. Mårtensson, L. Samuelsson, and W. Seifert, J. Phys. Chem. B **109**, 13567 (2005).

[19] R. K. Debnath, R. Meijers, T. Richter, T. Stoica, R. Calarco, and H. Lüth, Appl. Phys. Lett. **90**, 123117 (2007).

[20] K. A. Bertness, A. Roshko, L. M. Mansfield, T. E. Harvey, and N. A. Sanford, J. Cryst. Growth **310**, 3154 (2008).

[21] L. Largeau, D. L. Dheeraj, M. Tchernycheva, G. E. Cirlin, and J.-C. Harmand, Nanotechnology **19**, 155704 (2008).

[22] R. Songmuang, T. Ben, B. Daudin, D. González, and E. Monroy, Nanotechnology **21**, 295605 (2010).

[23] C. Chèze, L. Geelhaar, A. Trampert, and H. Riechert, Appl. Phys. Lett. **97**, 153105 (2010).

[24] S. D. Carnevale, J. Yang, P. J. Phillips, M. J. Mills, and R. C. Myers, Nano Lett. **11**, 866 (2011).

[25] R. Mata, K. Hestroffer, J. Budagosky, A. Cros, C. Bougerol, H. Renevier, and B. Daudin, J. Cryst. Growth **334**, 177 (2011).

[26] C. T. Foxon, S. V. Novikov, J. L. Hall, R. P. Campion, D. Cherns, I. Griffiths, and S. Khongphetsak, J. Cryst. Growth **311**, 3423 (2009).

[27] E. Galopin, L. Largeau, G. Patriarche, L. Travers, F. Glas, and J.-C. Harmand, Nanotechnology **22**, 245606 (2011).

[28] R. Calarco, R. J. Meijers, R. K. Debnath, T. Stoica, E. Sutter, and H. Lüth, Nano Lett. **7**, 2248 (2007).

[29] T. Gotschke, T. Schumann, F. Limbach, T. Stoica, and R. Calarco, Appl. Phys. Lett. **98**, 103102 (2011).

[30] V. Consonni, A. Trampert, L. Geelhaar, and H. Riechert, Appl. Phys. Lett. **99**, 033102 (2011).

[31] V. G. Dubrovskii, N. V. Sibirev, G. E. Cirlin, I. P. Soshnikov, W. H. Chen, R. Larde, E. Cadel, P. Pareige, T. Xu, B. Grandidier, J.-P. Nys, D. Stievenard, M. Moewe, L. C. Chuang, and C. Chang-Hasnain, Phys. Rev. B **79**, 205316 (2009).

[32] V. G. Dubrovskii, N. V. Sibirev, G. E. Cirlin, A. D. Bouravleuv, Yu. B. Samsonenko, D. L. Dheeraj, H. L. Zhou, C. Sartel, J.-C. Harmand, G. Patriarche, and F. Glas, Phys. Rev. B **80**, 205305 (2009).

[33] V. G. Dubrovskii, I. P. Soshnikov, N. V. Sibirev, G. E. Cirlin, V. M. Ustinov, M. Tchernycheva, and J.-C. Harmand, Semiconductors **41**, 865 (2007).

[34] V. G. Dubrovskii and N. V. Sibirev, J. Cryst. Growth **304**, 504 (2007).

[35] V. G. Dubrovskii, T. Xu, Y. Lambert, J.-P. Nys, B. Grandidier, D. Stiévenard, W. Chen, and P. Pareige, Phys. Rev Lett. **108**, 105501 (2012).

[36] V. G. Dubrovskii, V. Consonni, A. Trampert, L. Geelhaar, and H. Riechert, Appl. Phys. Lett. **100**, 153101 (2012).

[37] V. Consonni, M. Knelangen, A. Trampert, L. Geelhaar, and H. Riechert, Appl. Phys. Lett. **98**, 071913 (2011).

[38] P. Dogan, O. Brandt, C. Pfüller, A.-K. Bluhm, L. Geelhaar, and H. Riechert, J. Cryst. Growth **323**, 418 (2011).

[39] L. Lymperakis and J. Neugebauer, Phys. Rev. B **79**, 241308(R) (2009).

[40] P. Hacke, G. Feuillet, H. Okumura, and S. Yoshida, Appl. Phys. Lett. **69**, 2507 (1996).

[41] S. Guha, N. A. Bojarczuk, and D. W. Kisker, Appl. Phys. Lett. **69**, 2879 (1996).

[42] G. Koblmüller, R. Averbeck, H. Riechert, and P. Pongratz, Phys. Rev. B **69**, 035325 (2004).

[43] L. He, Y. T. Moon, J. Xie, M. Muñoz, D. Johnstone, and H. Morkoç, Appl. Phys. Lett. **88**, 071901 (2006).